

Neurofilament light chain and dorsal root ganglia injury after adeno-associated virus 9 gene therapy in nonhuman primates

Eric W. Johnson,¹ Jeffrey J. Sutherland,¹ Emily Meseck,² Cameron McElroy,² Deepa H. Chand,^{2,3} Francis Fonyuy Tukov,² Eloise Hudry,¹ and Kelley Penraat¹

¹Novartis Institutes for BioMedical Research, Cambridge, MA 02139, USA; ²Novartis Pharmaceuticals Corporation, East Hanover, NJ 07936, USA; ³University of Illinois College of Medicine–Peoria, Children’s Hospital of Illinois, Peoria IL 61605, USA

In nonhuman primates (NHPs), adeno-associated virus serotype 9 (AAV9) vectorized gene therapy can cause asymptomatic microscopic injury to dorsal root ganglia (DRG) and trigeminal ganglia (TG) somatosensory neurons, causing neurofilament light chain (NfL) to diffuse into cerebrospinal fluid (CSF) and blood. Data from 260 cynomolgus macaques administered vehicle or AAV9 vectors (intrathecally or intravenously) were analyzed to investigate NfL as a soluble biomarker for monitoring DRG/TG microscopic findings. The incidence of key DRG/TG findings with AAV9 vectors was 78% (maximum histopathology severity, moderate) at 2–12 weeks after the dose. When examined up to 52 weeks after the dose, the incidence was 42% (maximum histopathology severity, minimal). Terminal NfL concentrations in plasma, serum, and CSF correlated with microscopic severity. After 52 weeks, NfL returned to pre-dose baseline concentrations, correlating with microscopic findings of lesser incidence and/or severity compared with interim time points. Blood and CSF NfL concentrations correlated with asymptomatic DRG/TG injury, suggesting that monitoring serum and plasma concentrations is as useful for assessment as more invasive CSF sampling. Longitudinal assessment of NfL concentrations related to microscopic findings associated with AAV9 administration in NHPs indicates NfL could be a useful biomarker in nonclinical toxicity testing. Caution should be applied for any translation to humans.

INTRODUCTION

Spinal sensory or dorsal root ganglia (DRG) and trigeminal ganglia (TG) microscopic findings, often referred to collectively as DRG toxicity, have emerged in association with adeno-associated virus (AAV) gene therapies administered systemically or to the cerebrospinal fluid (CSF) in nonclinical studies involving nonhuman primates (NHPs), rats, and mini-pigs.^{1–4} The described microscopic findings are heterogeneously distributed across multiple DRG and/or TG within each animal. In most cases, such microscopic lesions remain clinically silent or asymptomatic in NHPs, outside the limits of detection of such sensory changes in this laboratory species in a nonclinical toxicology study setting, and potential translation to patients is uncer-

tain. In mini-pigs, clinical proprioceptive deficits have been observed in life that were associated with microscopic findings,² whereas clinical observations were reportedly rarely observed in rats, similar to NHPs.¹ As such, identifying and characterizing relevant soluble biomarkers as surrogates for monitoring AAV serotype 9 (AAV9)-related microscopic neuropathologic changes of the sensory ganglia would be valuable in nonclinical and clinical settings, albeit with different considerations and caveats in each of those settings.

Somatic sensory ganglia, such as the DRG, house the afferent somatic sensory neuronal cell bodies (soma) with pseudo-unipolar axons that bifurcate just after exiting the soma to innervate the dermis throughout the body via the distal process.^{5,6} The proximal process carries one of several diverse dermal sensory signals (e.g., pressure, heat, proprioception, nociception) to the spinal cord and/or brain within the dorsal (posterior) white matter tract (dorsal funiculus) of the spinal cord, terminating in the dorsal gray matter of the spinal cord and/or the brain stem (cuneate or gracilis nuclei).^{5,6} Sensory neurons in the DRG or TG are surrounded by satellite glial cells, scant numbers of resident tissue macrophages, and T and B lymphocytes supplied by a dense fenestrated vasculature that allows the passage of large and small molecules.^{7–10} Sensory neuronal cell body injury can lead to a range of outcomes, including neuron degeneration (potentially reversible injury), necrosis (cell death after irreversible injury), and/or loss (removal following cell death) and is frequently accompanied by activation of satellite glial cells, activation and infiltration of macrophages, infiltration and/or proliferation of T and B lymphocytes, and axonal degeneration extending into both the peripheral nervous system (PNS) and central nervous system (CNS).^{2,3,10–12} Cellular constituents released or produced as a result of the degenerative, necrotic, and/or inflammatory processes may be released into extracellular fluid and subsequently diffuse into the CSF and blood (serum and plasma), in which matrix can be collected, processed, and analyzed for the presence of these unique cellular

Received 19 September 2022; accepted 22 December 2022;
<https://doi.org/10.1016/j.omtm.2022.12.012>

Correspondence: Kelley Penraat, Novartis Institutes for BioMedical Research, 250 Massachusetts Avenue, Cambridge, MA 02139, USA.
E-mail: kelley.penraat@novartis.com



components, which can serve as surrogate biomarkers of cellular injury that are more sensitive than clinical observations or other nervous system endpoints, such as nerve conduction velocity. Ideally, these biomarkers represent a characteristic biological response within the tissue of interest. For neurodegenerative processes within the DRG, the purpose of a soluble biomarker in the context of a nonclinical study is detection of asymptomatic neuronal injury and/or accompanying inflammation that otherwise requires the terminal endpoint of microscopic evaluation, which cannot be applied longitudinally. The biomarker may also add information regarding the magnitude and time course of that injury, including resolution of the finding, which, in the absence of associated in-life observations, may otherwise go undetected without a complete autopsy or necropsy evaluation. The unique attributes and location of the DRG in the PNS—at the periphery of the CNS with access to CSF and with fenestrated vasculature surrounding neuronal cell bodies and axons extending into peripheral nerves—provide an opportunity for soluble biomarker assessment in peripheral whole blood using serum or plasma. Further, because DRG axons extend into the spinal cord tracts, sampling of the CSF may also be informative.

Soluble biomarker assays for neuroaxonal injury and inflammation have recently become more useful in nonclinical and clinical settings because of the development of more sensitive electrochemiluminescence and single-molecule array assay methods.^{13,14} Increased assay sensitivity allows biomarkers to be analyzed in peripheral blood matrices, as well as CSF, the latter of which generally has greater analyte concentrations. For example, single-molecule array, electrochemiluminescence, and enzyme-linked immunosorbent assay methods have published sensitivities of 0.62 pg/mL, 15.6 pg/mL, and 78 pg/mL, respectively, for neurofilament light chain (NfL), making only single-molecule array applicable for measurement of NfL in serum because of lower concentrations found in blood compared with CSF.¹⁵ Recently, biomarker panels that use the more sensitive single-molecule array assay methods have been developed for assessment of neuron injury and inflammation. Biomarkers commonly used for neurodegenerative investigations include NfL, glial fibrillary acidic protein (GFAP), ubiquitin C-terminal hydrolase, Tau, and neurofilament heavy chain (NfH).^{1,14,16} In several early nonclinical studies (not published), neopterin, ubiquitin C-terminal hydrolase, Tau, GFAP, and NfL were assessed, and NfL results were the most consistent and sensitive in our laboratory. Therefore, we focused our investigative efforts on NfL, a subunit of neurofilament and one of several cytoskeletal intermediate filaments (approximately 10 nm in diameter) that provides structural support, regulates axonal diameter, and is present in all neurons, including the DRG of humans and animals.^{1,9,14} In addition, neuronal injury leads to the diffusion of neurofilaments into the extracellular fluid and subsequently into the blood and CSF in humans and animals.¹⁷ NfL is the most abundant intermediate filament and forms the neurofilament core on which neurofilament medium (NfM) and NfH chains combine. Increases in NfL concentrations have been used as indicators of neuroaxonal injury and have recently been reported to be useful in the monitoring of AAV-induced DRG injury in NHPs and rats.^{1,13,14} NfL transcriptional and proteomic expression profiles confirm the presence of NfL

in the DRG of NHPs,¹ which is consistent with our internal investigation demonstrating strong immunohistochemical NfL staining of the neuronal cell bodies and the axons of the NHP DRG.

This meta-analysis describes the performance of NfL on the single-molecule array platform in relation to the incidence and severity of asymptomatic DRG microscopic findings associated with one-time dose of AAV9 gene therapies in cynomolgus macaques by intravenous (i.v.) and intrathecal (IT) routes (lumbar puncture [LP] or intra-cisterna magna [ICM] injection) of administration.

RESULTS

In-life observations

An extremely low incidence of clinical signs related to DRG microscopic findings was observed, with only 1 of 193 AAV9-dosed cynomolgus macaques (0.5%) demonstrating combined sensory and motor neurologic clinical findings on day 20 after the dose. The affected animal was administered the greatest study dose of a vector at 4×10^{13} vg/animal IT-LP on study day 1 that encoded a transgene that is present at greater (physiologic) concentrations in the neurons of non-diseased (wild-type, clinically normal) animals and that is known to be neurotoxic when expressed at supraphysiologic concentrations. In-life observations in this single animal included decreased tail tone, a weak or parietic gait, hunched posture, and bilateral lumbar scabs, which led to early euthanasia 20 days after IT administration. Iatrogenic injury of the spinal cord was considered, but discarded as an explanation of the clinical findings, and test article-related microscopic findings in this animal included findings in the DRG and the spinal cord (neuronal degeneration of the ventral motor neurons and degeneration of axons in the ventral and ventrolateral spinal cord white matter), consistent with the in-life clinical observations and not limited to the typical DRG microscopic findings described in literature in macaques, which are generally asymptomatic.²⁻⁴ The cause of moribund condition was skin inflammation associated with bilateral lumbar scabs, which was attributed to altered skin sensation-related microscopic findings of neuron degeneration and mononuclear cell inflammation in the DRG and axonal degeneration of the dorsal spinal nerve root. Excluding this complex case, which had microscopic findings in more than just the DRG, no macaques had sensory abnormalities associated with DRG microscopic findings.

DRG microscopic evaluation (histopathology)

Consistently throughout the nine nonclinical toxicity studies, spanning scheduled necropsy time points of 2–52 weeks after IT infusion (LP or ICM) of AAV9 vectorized genome constructs ranging from 4.8×10^{12} vg/animal to 9.2×10^{13} vg/animal or i.v. infusion of 1×10^{14} vg/kg, there were microscopic findings of neuronal degeneration, necrosis, and/or neuronal cell body loss (recorded under aggregates, satellite glial cells/neuronal cell loss) (Table S1, Figure 1). Notably, microscopic findings were of lower incidence and severity (limited to minimal or slight severity) at the 52-week time point. Concomitant or secondary axonal degeneration in the spinal cord (dorsal white matter tract or dorsal funiculus) and peripheral nerves were primarily observed at time points from 2–12 weeks after the dose, with a relative dearth of these

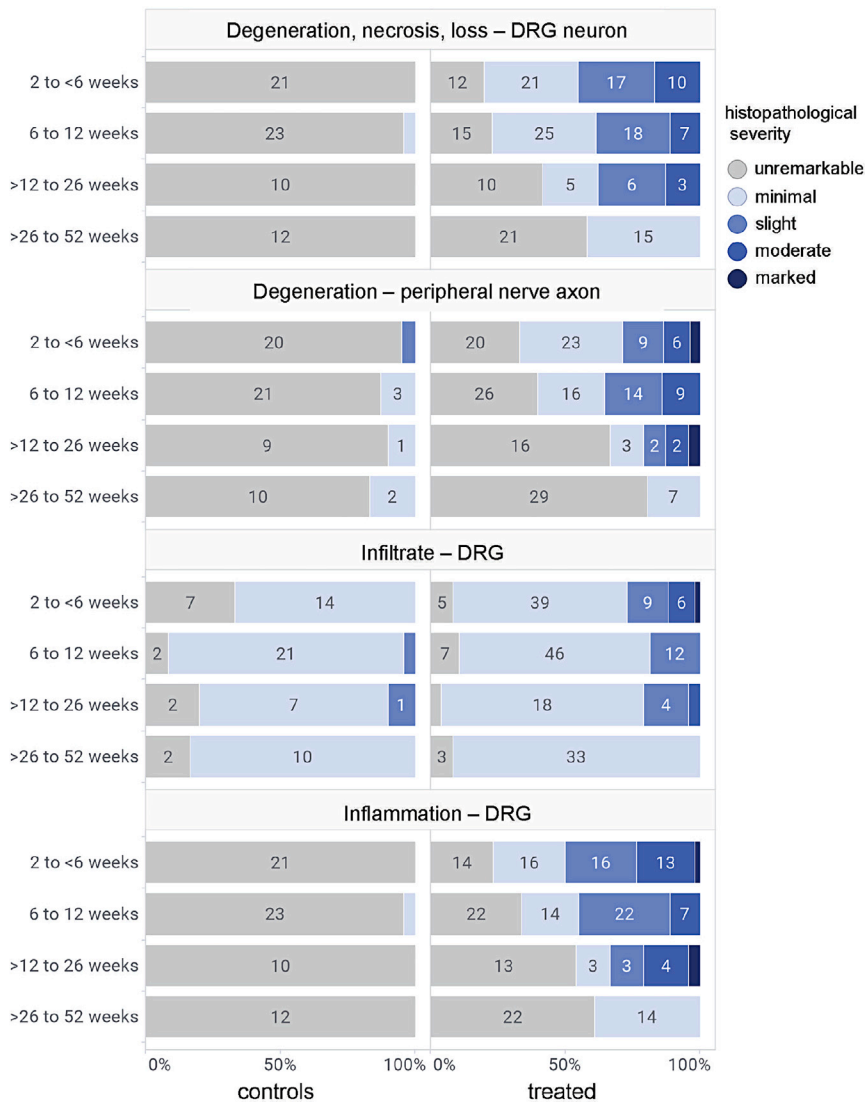


Figure 1. Incidence of histology findings according to study period

Summary of representative DRG histology finding incidence by study duration across 67 control (left) versus 185 treated (right) cynomolgus macaques; eight animals receiving empty capsid or promoter-less transgene constructs were excluded; bar width is scaled to present the percentage of cynomolgus macaques by maximum severity; values on bars present the count of cynomolgus macaques at each severity.

in the magnitude of infiltrative inflammatory cells between test articles was observed, and the GFP reporter gene was not consistently the most inflammatory transgene product. Relatively little or no discernible dose response was reported in the DRG microscopic findings during this range of time points. More consistently, lumbar or sacral spinal sensory ganglia (DRG) were more severely affected compared with thoracic ganglia, whereas cervical ganglia microscopic severity was more variable (see [Table S2](#)).

Microscopic findings that were considered secondary to the neuronal cell body and sensory ganglia inflammatory changes included minimal to marked (marked limited to vectors encoding for a foreign GFP transgene) axon degeneration in the adjacent spinal root and/or spinal nerve ([Figure 1](#)). A background finding of mononuclear cell infiltrate was observed in all groups, including controls, in the ganglia, nerve roots, and peripheral nerves ([Figure 1](#)).

There was modest variation in the incidence and severity of DRG microscopic degeneration, necrosis, and/or loss with the various tested

AAV9 promoter-transgene test articles, but the incidence and severity did not demonstrate a dose relationship in terminal time points up to 12 weeks.

Later DRG microscopic findings (>12–52 weeks after the dose)

After approximately 52 weeks of observation of a one-time IT-LP or IT-ICM dose, microscopic sensory ganglia (DRG and/or TG) findings were limited to minimal or slight severity neuronal degeneration, mononuclear cell inflammation, and/or satellite glial cell aggregates, which was interpreted to reflect normal tissue remodeling in the form of a scar following removal of the degenerate or necrotic neuron ([Figure 1](#)). Associated findings of axon degeneration in dorsal white matter tract or dorsal funiculus and in the peripheral nerves were absent, further indicating resolution of the peripheral findings and supporting a lack of ongoing or progressive injury or findings in the DRG. A summary of all findings across

findings at 52 weeks, supporting that the DRG findings were not progressive at this later time point ([Figure 1](#)). Neurodegeneration or necrosis were not (or rarely) observed in either spinal cord motor neurons or neurons within the brain parenchyma. No DRG microscopic findings were observed in cynomolgus macaques administered empty AAV9 capsid or self-complementary AAV9 (scAAV9) promoter-less transgene construct ([Table S1](#), [Figure S1](#)).

Early DRG microscopic findings (2–12 weeks after the dose)

AAV9-related microscopic findings in the DRG examined approximately 2–12 weeks after the IT dose were characterized primarily by somewhat randomly distributed minimal to moderate neuronal degeneration, necrosis, and/or loss, minimal to moderate mononuclear cell inflammation, and/or minimal to slight increased satellite glial cells. Compared with later time points, mononuclear cell inflammation was more prominent when assessed between 2 and 12 weeks. Variation

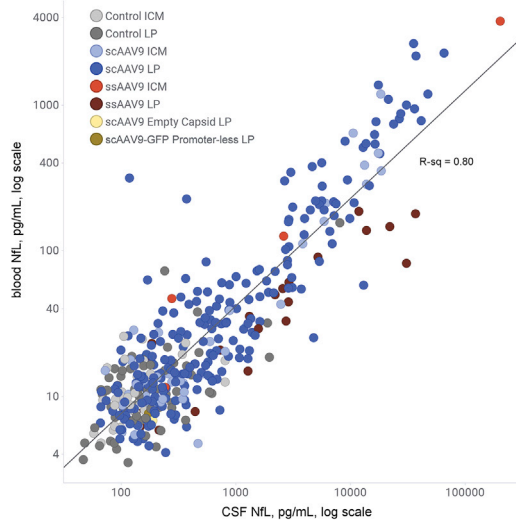


Figure 2. Comparison of blood and CSF NfL concentrations

Comparison of blood (serum and plasma) versus CSF NfL concentrations across 399 paired samples for which blood and CSF sampling were performed on the same study day. scAAV9, self-complementary AAV9; ssAAV9, single-stranded AAV9.

treatment groups categories is provided in [Table S3](#) and animal-level diagnoses in [Table S2](#).

Meta-analysis of DRG-selected microscopic finding incidence and severity

The incidence of microscopic DRG neuron degeneration, necrosis, and/or loss in cynomolgus macaques administered AAV9-promoter-gene test article was 78%, with a maximum severity for each animal that ranged from minimal to moderate from approximately 2–12 weeks. In comparison, after 52 weeks of observation, the incidence of microscopic, asymptomatic DRG neuron degeneration, necrosis, and/or loss in cynomolgus macaques administered AAV9-promoter gene constructs was 42%, with a maximum severity of minimal for each terminal necropsy animal. This decrease in severity and incidence supports interpretations that the asymptomatic neuronal degenerative change observed microscopically was not progressive and that the lower incidence and/or severity at 52 weeks of observation was evidence of resolution, if not reversibility, of these microscopic findings.

Timeline of NfL changes and correlation between CSF and plasma NfL concentrations

Neuronal cell bodies and the axons were positive for NfL with immunohistochemical staining, confirming the presence of this intermediate filament in the DRG of NHP ([Figure S2](#)). NfL measurable assay results ranged from 0.416 to 415 pg/mL, with an average intra-assay precision of 6%, 11%, and 11% for serum, plasma, and CSF, respectively. The average recovery of spiked NfL at three concentrations (low, medium, and high) was 102%, 159%, and 114% in serum, plasma, and CSF, respectively. The bias noted with each matrix was

constant over the range of concentrations tested. The 95% confidence interval (CI) for all pre-dose values ranged from 11.2 to 13.3 pg/mL in serum (N = 253; mean = 12.2 pg/mL), 10.4–14.0 pg/mL in plasma (N = 73; mean = 12.2 pg/mL), and 165–219 pg/mL in CSF (N = 184; mean = 192 pg/mL). The 95% CI for all post-dose vehicle control samples ranged from 13.6 to 35.1 pg/mL in serum (N = 169; mean = 24.3 pg/mL), 12.8–16.9 pg/mL in plasma (N = 120; mean = 14.9 pg/mL), and 104.8–762.6 pg/mL in CSF (N = 118; mean = 433.7 pg/mL) ([Table S4](#)).

Blood NfL concentrations were well correlated with CSF concentrations (Pearson $R^2 = 0.80$; N = 399) ([Figure 2](#), [Table S5](#)). When examined individually, CSF versus serum ($R^2 = 0.80$; N = 311) and CSF versus plasma ($R^2 = 0.82$; N = 88) were similar and within the range of values observed across studies. To normalize comparison between studies and matrices, all NfL assessments were normalized versus the last pre-dose measurement (i.e., fold change vs. pre-dose). The time course of changes in NfL concentrations in blood (serum and plasma) and CSF paralleled the histopathology findings in the DRG at both early (approximately 2–12 weeks) and late time points (>12 weeks) ([Figure 3](#)). Modest early elevations in blood NfL, compared with pre-test and control readings, were reported in several studies starting on 8 days after AAV9 IT administration, generally reaching maximum concentrations between 15 and 28 or 29 days after the dose and decreasing thereafter ([Figure S3](#)).

Correlation between NfL changes and DRG histopathology findings

The transient elevation of blood (serum and plasma) and CSF NfL concentrations was similar to the time-dependent variation in the incidence and severity of DRG microscopic findings (injury) observed via histopathology. To assess the usefulness of NfL as a soluble biomarker for DRG injury, terminal NfL measurements in blood (serum and plasma) and CSF were compared with the composite DRG endpoint (see [materials and methods](#)) ([Table S6](#)). The distribution of absolute or fold change from the pre-dose for NfL concentrations in blood and CSF were positively correlated with lesion grade ([Figures 4](#) and [S4](#)). NfL measures from 207 animals with results across all four NfL measures suggest similar usefulness in differentiating animals by DRG histology outcome ([Table 1](#)). Excluding animals with DRG injury grade of minimal increased receiver operating characteristic (ROC) area under the curve (AUC) ([Figure 5A](#) and [5B](#)), this is consistent with improved biomarker performance when setting aside ambiguous outcomes according to histopathology.

The correlation between each animal's NfL concentration and DRG injury may be confounded by other study parameters (e.g., receiving a vehicle treatment or receiving a greater treatment dose). Outcomes for the composite histology endpoint were classified as positive for DRG injury (grade of minimal and above) versus negative (unremarkable) and used for training a logistic regression model. To assess the usefulness of NfL in predicting injury beyond potential confounders, we compared two models: the first containing only potential confounders (dose, route, sex, belonging to a treatment group) as

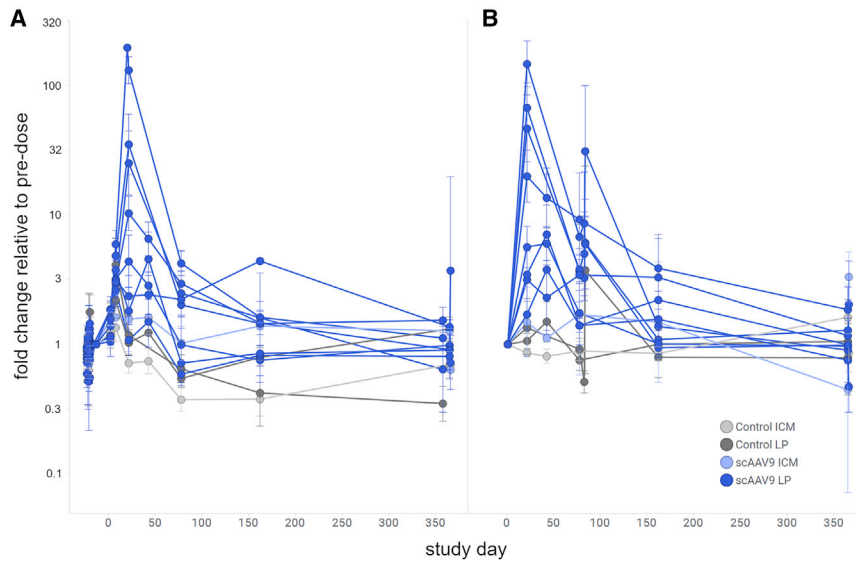


Figure 3. Changes in NfL concentrations in blood and CSF

Time course of changes in NfL concentrations in (A) blood (serum) and (B) CSF NfL in three studies of 52 weeks duration after the dose. Each line represents 1 of 12 treatment groups across the studies (4 groups per study, including 1 control group). Error bars are standard error of the mean, calculated on a log scale.

predictors and the second containing the confounders and blood NfL ratio. Adding blood NfL ratio significantly improved model fit ($p = 8 \times 10^{-11}$; χ^2 test), suggesting that its usefulness in predicting DRG injury extends beyond the confounders.

Because NfL concentrations in blood and CSF are correlated and may explain the same variation in DRG injury risk, we compared a logistic regression model using the blood NfL ratio alone with a model using both blood and CSF ratios. Addition of the CSF ratio improved the model compared with blood ratio alone ($p = 0.0003$; χ^2 test). Comparing model response versus DRG injury class revealed a modest difference in predictive accuracy: ROC AUC = 0.83 for the model using only blood NfL ratio, and ROC AUC = 0.85 for the model using both blood and CSF ratios (Figure 5C). Taken together, these results suggest that blood NfL concentrations are sufficient for monitoring potential DRG injury, with lesser benefit from adding CSF concentrations to the risk assessment.

Biomarkers of tissue injury are typically applied with a cutoff, which is used to identify degrees above which the probability of observing tissue damage via histology assessment is increased. The selected cutoff may depend on the nature of an application (e.g., varying tolerance of false-positive risk vs. false-negative risk). Table 2 provides assay sensitivity and specificity at several potential cutoffs, demonstrating the usefulness of the assay under the conditions of a nonclinical study setting. A cutoff of 1.5-fold in NfL from pre-dose values leads to the greatest sensitivity (including more true-positive correlations with DRG toxicity).

DISCUSSION

Neurofilaments belong to a class of intermediate filaments that comprise the principal structural components of neurons and axons, including neurons of the DRG.^{9,14} In addition, NfL transcriptomic and proteomic expression profiles confirm the presence of NfL in

the DRG of NHPs,¹ which is consistent with our internal investigation demonstrating immunohistochemical NfL staining of the neuronal cell bodies and the axons of the NHP DRG (Figure S2). Of the subunits that compose neurofilaments (NfH, NfM, NfL, α -internexin, and peripherin), NfL is the most abundant component, forming the intermediate filament core of neurons and axons.^{17,18} NfL is released from injured neurons to the extracellular fluid and diffuses into blood (serum and plasma)

and CSF and has been used to monitor patients and animals with neurologic lesions, including injury to sensory neurons in DRGs, in a variety of diseases such as Alzheimer's disease, Guillain-Barré syndrome, oxaliplatin-induced peripheral neuropathy, Friedreich's ataxia, and AAV-induced DRG injury.^{1,14,19–24} NfL concentrations have also demonstrated increases before clinical manifestation of symptoms related to disease onset, making this biomarker an interesting candidate for use in drug development to monitor safety liabilities.¹⁶

In this investigation of AAV9-induced DRG injury in cynomolgus macaques, the high-sensitivity single-molecule array Quanterix human NfL assay performed well in cynomolgus macaque matrix with a wide measurable assay range of 0.416 to 415 pg/mL with low imprecision and acceptable recovery in serum, plasma, and CSF. The mean pre-dose concentration of CSF NfL was 16 times greater compared with blood (serum and plasma) NfL concentrations in naive cynomolgus macaques, which is consistent with reports by Kuhle et al.¹⁵ The pre-dose biologic range was narrow in blood (<5 pg/mL) and CSF (<140 pg/mL) for naive cynomolgus macaques. However, the biologic range of both blood (serum and plasma) and CSF NfL in naive vehicle-control cynomolgus macaques during study conduct, after vehicle administration, was greater and generally wider than pre-dose samples. The slightly greater NfL concentrations with wider biologic ranges in vehicle control animals and animals with unremarkable DRG findings and elevated NfL during study conduct were likely a reflection of study-related procedures such as IT or i.v. dose administration, femoral vein blood collection methods, interaction between co-housed animals, and/or animal handling methods, since NfL is a sensitive indicator of neuronal injury. This is consistent with a report that demonstrated that cerebrospinal neurofilament concentrations can remain elevated for up to 3 weeks after IT-LP procedures in NHPs.²⁵ In addition, because of the relative heterogeneity

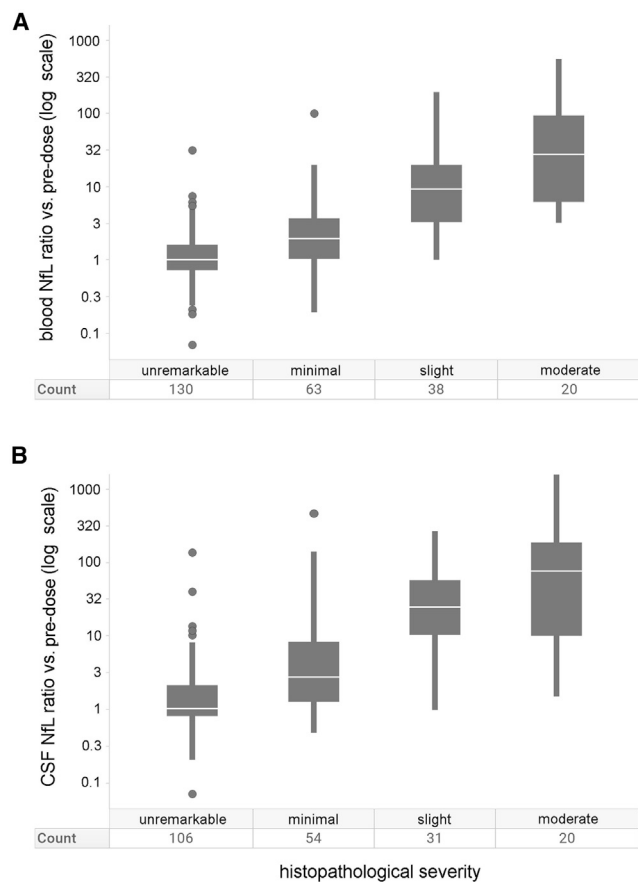


Figure 4. Blood and CSF ratios according to severity of DRG findings

Distribution of blood (A, serum and plasma) and (B) CSF measured as fold change from pre-dose by maximum severity grade of DRG finding (degeneration, necrosis, and/or loss – neuron).

of the lesion and because not all DRGs from all animals administered AAV were examined microscopically, it is possible that an increase in NfL (which is representative of all DRGs) may not have been associated with microscopic changes. Therefore, care must be used in the design and interpretation of biomarker studies in relation to study procedures, collection time points, and methods.

The terminal changes in blood (serum and plasma) and CSF NfL compared with pre-dose values correlated with the incidence and severity grade of DRG findings of neuron degeneration, necrosis, and/or loss with post-dose observation periods of up to 52 weeks, with the peak NfL concentrations observed before 12 weeks after the dose. In addition, both absolute and fold changes from pre-dose of blood and CSF NfL correlated well with the severity of the histologic scores of maximum degeneration, necrosis, and/or loss at both early (approximately 2–12 weeks) and late (>12 weeks) time points. Blood (serum and plasma) NfL concentrations were well correlated with CSF concentrations with R^2 values of 0.8, suggesting that non-invasive blood sampling methods could be used for NfL monitoring of

Table 1. Correlation of blood (serum and plasma) and CSF measures of NfL versus the DRG composite endpoint

	Kendall Tau	ROC AUC ^{a,c}	ROC AUC, no minimal ^{b,c}
blood, NfL (pg/mL)	0.55	0.85	0.95
blood, NfL fold change from pre-test	0.54	0.83	0.96
CSF, NfL (pg/mL)	0.50	0.81	0.94
CSF, NfL fold change from pre-test	0.51	0.83	0.94

^aUsing 207 animals with all measures defined and a DRG assessment performed.

^bExcluding animals with minimal grade (i.e., comparing “unremarkable” vs. “slight” or “moderate” grades).

^cROC AUC values differ from Figure 5 because only the subset of animals with all NfL measures was used in this comparison.

DRG-related injury. The ROC with blood and CSF NfL versus pre-dose ROC AUC values were good (0.82 and 0.83, respectively) for distinguishing a maximum severity score of more than 1 (minimal) for DRG injury and excellent (0.95 and 0.95, respectively) for distinguishing a maximum severity score of 2 or more (slight) for DRG injury under the rigorously controlled conditions of nonclinical study conduct in cynomolgus macaques.

No increases in NfL were observed within a 28-day post-dose observation period after administration of empty AAV9 capsid and scAAV9 containing a promoter-less transgene, consistent with the subsequent lack of DRG degeneration, necrosis, and/or loss, supporting the supposition that the pathogenesis of the AAV-related DRG injury and inflammation is driven by increased transgene expression regulated by the promoter used.^{26,27}

The incidence of clinical signs related to the DRG microscopic findings was 0.5% (1/185 animals treated with full AAV9 vector). The affected animal was intrathecally administered the greatest study dose of the AAV9 recombinant vector (4×10^{13} vg/animal), leading to the expression of a transgene known to be neurotoxic when expressed at supraphysiologic concentrations in non-diseased (clinically normal) animals. This animal had the greatest serum NfL concentration in the study on day 20 at the time of terminal collection. In-life observations of this single animal included decreased tail tone, a weak or parietic gait, hunched posture, and bilateral lumbar scabs and led to early euthanasia of this animal 20 days after the one-time dose administration. The mixture of sensory and motor neurologic clinical findings demonstrated 20 days after the dose was specific to the payload used in this particular study and, therefore, is not expected to be generalized to other transgenes.

The scAAV9-related microscopic findings in the DRG of NHPs examined at scheduled necropsy approximately 2–12 weeks after the one-time IT or i.v. administration included minimal to moderate neuronal degeneration, necrosis, and/or loss to neurons; minimal to moderate mononuclear cell inflammation; and/or minimal to slightly

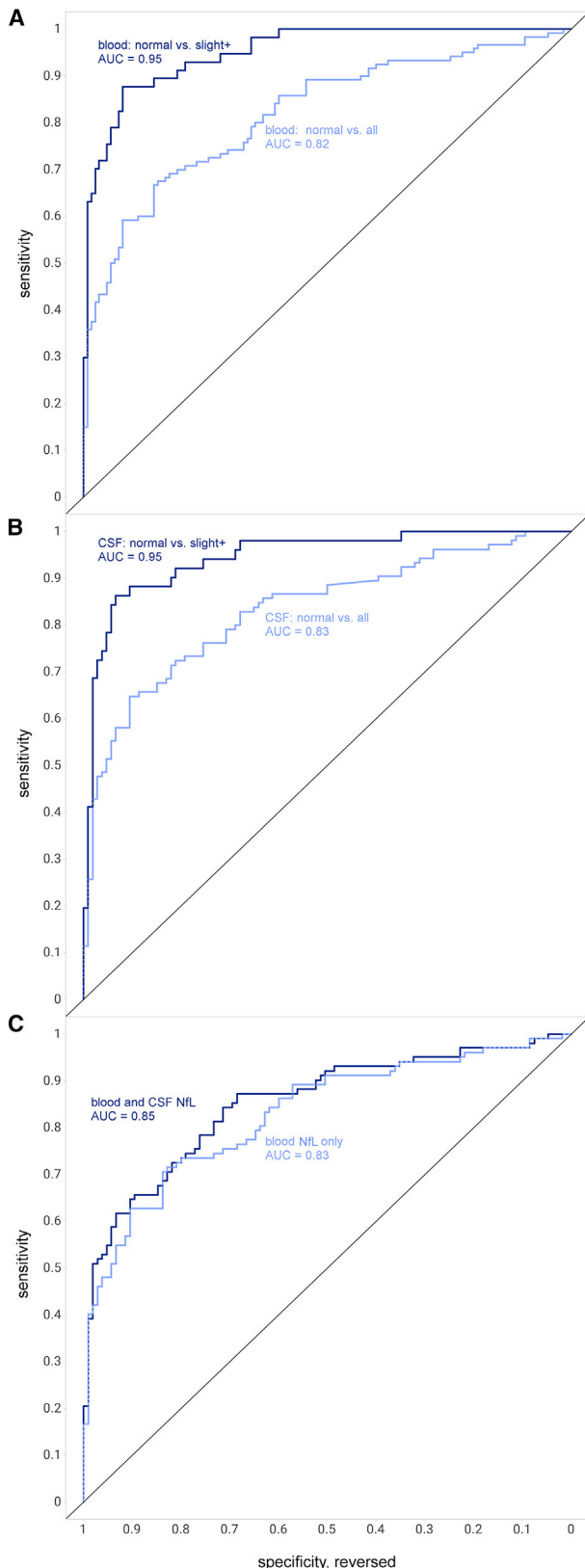


Figure 5. ROC AUC analysis of NfL concentrations versus the DRG composite endpoint

ROC AUC analysis comparing NfL concentrations versus DRG composite endpoint. AUC for comparison of unremarkable versus all (light blue lines) or unremarkable versus slight or moderate (dark lines) for (A) blood NfL versus pre-dose (ROC AUC values of 0.82 and 0.95) and (B) CSF NfL versus pre-dose (ROC AUC values 0.83 and 0.95). (C) ROC AUC analysis comparing logistic regression model predictions versus DRG outcome (unremarkable vs. all) using blood NfL alone (light blue; AUC = 0.83) versus model using blood and CSF NfL (dark blue; AUC = 0.85).

increased satellite glial cells (characterized by more and larger satellite glial cells in areas of neuronal injury/inflammation). Secondary findings included minimal to marked (marked severity was limited to scAAV9-CMV-GFP) axon degeneration in the adjacent spinal root and/or spinal nerve associated with the DRG sensory neurons, with a lack of injury to other neuronal and axonal populations in the CNS and PNS despite extensive sampling. Mononuclear cell infiltrate without corresponding injury to neurons was observed in all groups, including controls. The incidence of DRG degeneration, necrosis, and/or loss after a one-time IT (4.8×10^{12} to 9.2×10^{14} vg/animal) or i.v. (1.0×10^{14} vg/kg) administration with scAAV9 promoter transgene construct (test article) was 78% (maximum histopathology severity, moderate) at 2–12 weeks after the dose.

At observation (necropsy) time points of 12 weeks to 52 weeks after the dose, microscopic findings in DRG tissue were limited to minimal to slight neuronal degeneration, mononuclear cell inflammation, and/or satellite glial cell aggregates. The incidence of DRG degeneration, necrosis, and/or loss after the one-time IT (1.2×10^{13} to 9.2×10^{13} vg/animal) administration of scAAV9 + promoter + transgene construct (test article) was decreased to 42% (maximum severity, minimal) at time points up to 52 weeks after the dose, with a trend toward resolution of the findings reported after week 12.

The DRG finding results presented here are similar to Hordeaux et al.³ and support examination of DRG in nonclinical studies at interim time points before 12 weeks and terminal time points after 12 weeks, representing NHP platform-related findings observed with AAV gene therapies. Thus far, in NHPs, lesions are generally asymptomatic and have not yet been generally recognized in clinical development.

Overall, NfL performed well under the conditions of these nonclinical studies in relation to monitoring of AAV-induced DRG injury. These findings are consistent with a published report of a small number of NHPs in a short-duration study.¹ The current meta-analysis provides a more comprehensive review by including nine studies with 260 animals over 52 weeks, following the time course of both NfL concentrations and microscopic DRG findings. In cynomolgus macaques, there seems to be correlation between the transient NfL increase and the onset of generally asymptomatic microscopic DRG findings that are considered nonprogressive, with a subsequent decrease in NfL concentrations and a trend toward the resolution of microscopic DRG findings in the nonclinical experimental setting.

Table 2. Assay performance characteristics when employing NfL ratio as a biomarker of DRG injury

Cutoff (fold)	Blood		CSF	
	Sensitivity	Specificity	Sensitivity	Specificity
1.5	0.73	0.71	0.83	0.68
2	0.68	0.82	0.76	0.72
3	0.59	0.92	0.68	0.84
5	0.43	0.96	0.60	0.91
10	0.32	0.99	0.49	0.95

DRG injury was categorized as positive (minimal and greater) versus negative (unremarkable) on the same composite endpoint of DRG neuron injury used throughout this work.

Therefore, NfL may be useful as an exploratory soluble biomarker for monitoring DRG injury in NHPs after AAV administration.

To date, NfL measurements have not been incorporated into clinical trials for AAV therapies. The correlation with respect to clinical manifestations, histopathologic DRG toxicity, and serum NfL measurements has yet to be verified in humans. However, data from Alves et al.²⁸ seem to have demonstrated similar transient increases of blood NfL from baseline with subsequent decreases for patients with spinal muscular atrophy administered a one-time i.v. dose of onasemnogene abeparvovec, as also observed in our NHP AAV9 gene therapy platform studies. Despite transient early post-dose increases in blood NfL, the children who were treated with gene therapy continued to achieve important efficacy motor milestones.²⁹ In addition, onasemnogene abeparvovec has demonstrated efficacy in thousands of patients with spinal muscular atrophy with no evidence of clinically relevant correlates to DRG (sensory neuronal) toxicity based on thorough analyses of clinical data from Phase III trials of onasemnogene abeparvovec.²⁹ The data presented by Alves et al.²⁸ suggest that NfL could be considered on an exploratory basis with baseline and longitudinal time course sampling to monitor patients receiving AAV-based therapies that target neurodegenerative diseases with background DRG injury when placed in the context of clinically relevant disease milestones.

Soluble biomarkers represent a characteristic biologic response within the tissue of interest. For the neurodegenerative processes within the DRG, the purpose of the biomarker is detection of asymptomatic neuronal injury that can add information regarding the magnitude and time course of a biologic response to nonclinical, and possibly clinical, underlying events that may otherwise go undetected. NfL is constitutively released at lesser concentrations during normal physiologic processes such as neuronal growth, repair, and aging.³⁰ Greater concentrations of NfL can occur with neuronal injury and are not disease specific, which could make clinical application in the context of monitoring for DRG toxicity in the background of neurodegenerative diseases and other comorbidities challenging compared with assessment in healthy NHP nonclinical development studies.³¹ Based on the outcome of this meta-analysis, longitudinal time course sampling

in conjunction with appropriate clinical assessments are recommended to assist in interpreting asymptomatic transient elevations of NfL concentrations in blood and CSF associated with AAV-induced asymptomatic DRG injury. In addition, understanding possible confounding factors such as kinetics within biofluids, clearance, degradation, stage of disease or injury, variations with lifestyle, and age in both the nonclinical and clinical settings is needed for application.³¹

In summary, transient DRG injury and subsequent resolution were observed in NHPs with several different AAV9 constructs along with concurrent transient elevations in blood and CSF NfL concentrations that correlated with histopathologic findings of degeneration, necrosis, and/or loss. Blood or CSF NfL findings associated with i.v. or IT administration in cynomolgus macaques as reported here should be considered in the context of this nonclinical, non-disease test system, and appropriate caution should be applied for any potential translation to human patients.

MATERIALS AND METHODS

Animal test system

A meta-analysis was conducted to systematically assess DRG toxicity after AAV9 administration in NHPs. This meta-analysis aggregated data of 260 cynomolgus macaques (*Macaca fascicularis*) used across nine Good Laboratory Practice (GLP) and non-GLP toxicity studies: 193 animals were dosed with AAV9 viral vectors (including four animals administered empty capsid and four animals administered AAV9 viral vector with a promoter-less transgene), and 67 were dosed with vehicle material (tromethamine [20 mM], magnesium chloride [1 mM], sodium chloride [200 mM], and Poloxamer 188 [0.005%]; pH adjusted to 8.1 [\pm 0.1] with hydrochloric acid [6 M], Q.S. to volume with sterile water for injection, Tangential Flow Filtration [TFF] 3 buffer) and used as concurrent controls. Equal numbers of males and females were included in four GLP studies and one non-GLP study, whereas generally only one sex, based on animal availability, was used in the remaining four non-GLP studies. Ages of the cynomolgus macaques used in the nine studies ranged from 12 to 50 months (Table 3). All procedures were performed in compliance with the Animal Welfare Act, the Guide for the Care and Use of Laboratory Animals, and the Office of Laboratory Animal Welfare. Generally, Asian-origin primates from an accredited American supplier were used, but a small group of Mauritius-origin macaques from a European-based supplier were included in one non-GLP study. The portions of the studies conducted in-life were performed at one of two Labcorp Drug Development locations. Before study assignment, animals were preselected based on their anti-AAV9 antibody titer (total IgG). Only animals with an optical density of less than 0.4 and a ratio less than 2 at 1:50 dilution were included in the study.

AAV9 vectors and vehicle control

AAV9 vectors were used across all studies included in the analyses (Table 3). The genetic payloads of the vectors consisted of a self-complementary (eight studies) or single-stranded (one study) genome. Transgene expression was driven by the cytomegalovirus

Table 3. Overview of study details involving cynomolgus macaques (*Macaca fascicularis*)

	All	Male	Female
Total animals, n	260	107	153
Control, n	67	26	41
Administered AAV gene therapy, n	193	81	112
ROA: LP or ICM (vehicle or AAV9 at a dose of 4.8×10^{12} to 9.2×10^{13} vg/animal), n	224	89	135
ROA: i.v. (vehicle or AAV9 at a dose of $\sim 1.0 \times 10^{14}$ vg/kg), n	36	18	18
Age range	12–50 months		
Terminal time points	~2–52 weeks after single dose		
Blood collection time points for soluble biomarkers/NfL	Pre-test phase at least once and/or pre-dose day 1 followed by specific intervals during the in-life observation phase and within 1 week of terminal necropsy (including days 2, 7/8, 12/15, 22, 28/29, 43, 78, 162, and/or 358/365)		
CSF collection time points for soluble biomarkers/NfL	Pre-dose day 1 and/or at specific intervals during the in-life observation phase and at terminal necropsy (including days 8, 15, 22, 28/29, 43, 78, 162, and/or 365/366)		
NfL, neurofilament light chain; ROA, route of administration; vg, vector genomes.			

(CMV) early enhancer and a hybrid CMV enhancer/chicken β -actin promoter (CB promoter) in most instances, with the exception of three studies.

- In one GLP study, a short fragment of the methyl-CpG-binding protein 2 gene promoter (30 cynomolgus macaques) was used.
- In one non-GLP study, the human synapsin (hSYN) promoter (10 cynomolgus macaques) was used.
- In one GLP study, proprietary promoters (six cynomolgus macaques) were used.

Transgenes included human cDNA or the fluorescent reporter enhanced GFP gene. In one other study, promoter-less genetic cargo was packaged into AAV9 and empty AAV9 capsids that were used as test articles. The vectors used in these studies were produced using preclinical research standards (for GFP reporter genes, hSYN, and proprietary vectorized genome constructs) or Good Manufacturing Practice conditions (for GLP studies including the CB promoter with human cDNA). All viral lot material met acceptance and release criteria for *in vivo* research use for the percentage of empty capsid and total purity, number of process-related impurities, plasmid DNA or production cells, endotoxin concentrations (≤ 5.0 EU/mL), and osmolality. Dose formulations were prepared by diluting the respective drug substance in vehicle control article (TFF buffer) to target concentrations and testing per quantification method (droplet digital polymerase chain reaction).

Dosing procedures

IT dosing

On day 1, animals were anesthetized at the time of dosing with 10.0 mg/kg ketamine and 0.02 mg/kg dexmedetomidine. Animals were also administered an analgesic after the ketamine and dexmedetomidine but before the dosing procedure for IT-LP or before anesthesia for the IT-ICM dosing. In addition, animals dosed via IT-ICM were also administered a sustained-release nonsteroidal anti-inflammatory drug by subcutaneous injection. For two studies, a contrast agent (Omnipaque 180) was administered immediately before the AAV9 vectors (≤ 200 μ L, without exceeding a total volume of 2 mL) to be consistent with the intended clinical use and dose procedure. Up to 1 mL of CSF was withdrawn before administration at either location (IT-LP or IT-ICM). Directly after IT-LP dosing, the animals were maintained in dorsal recumbence with hind limbs elevated (Trendelenburg-like position) for at least 10 min after the completion of administration. Doses were infused via IT injection into the intervertebral space of L5–L6 (for at least 1 min) or the cisterna magna (for at least 2 min). Atipamezole (0.2 mg/kg for IT-LP dosing and 0.1 mg/kg for IT-ICM dosing) was administered as a reversal agent for the anesthesia at the end of the investigations.

i.v. dosing

AAV9 vectors or vehicle control articles were dosed by i.v. infusion via a saphenous vein (or alternatively via a cephalic vein) over approximately 20 min using a calibrated external infusion pump device.

In-life procedures

Clinical assessments

Clinical observations included (but were not limited to) twice-daily general observations, once-daily cage-side observations, detailed observations (at least weekly), weekly body weights, and qualitative daily food consumption determinations for all groups before dosing and during the observation period as indicated by the study protocol. Neurologic examinations by qualified and trained personnel were generally conducted during the pre-dose phase (at least twice), on days 1 and 2 (approximately 4 and 24 h after the dose, respectively), and intermittently thereafter until the end of the study. As part of the neurologic assessment, an examination of the head and eyes for unusual orientation and movements was performed. Reflexes, including menace, pupillary, palpebral, limb flexor, and patellar, were tested, and the muscle tone of unrestrained limbs was evaluated. Neurologic examinations also included assessments of locomotor activity, behavioral changes, coordination, posture, auditory startle response, characterization and/or the presence or absence of tremors or convulsions, and pupil evaluations.

CSF and blood collection and handling

CSF and blood collections were performed during the pre-test phase and/or on day 1, before dosing, at specific protocol-directed intervals during the in-life observation phase of each study, and on the day of scheduled euthanasia (Table 3). CSF sampling was performed in anesthetized animals through either the lumbar region or the cisterna magna. For each sample collected, a visual inspection was performed

to examine if the sample seemed to be contaminated with blood (pinkish appearance). If a sample seemed to be contaminated with blood, the spinal needle was repositioned for a second collection. Samples were held on wet ice or chilled cryoracks and centrifuged within 1 h of collection. The supernatant was harvested and stored at -60°C to -80°C until biomarker analyses were completed. Blood collection for soluble biomarkers was performed through the femoral or cephalic vein. Appropriate blood collection tubes were used (no additive or potassium [K2] ethylenediaminetetra-acetic acid [EDTA]). Samples were centrifuged within 1 h of collection of serum and/or plasma. Following harvesting, samples were stored at -60°C to -80°C until use. Both serum and plasma samples were obtained for each animal for analysis of the neuronal injury biomarker (NfL).

Terminal procedures

Animals underwent scheduled euthanasia or unscheduled necropsy (one animal). Nervous system sampling included collection and processing for light microscopic examination of at least five DRG from each of the cervical, thoracic, and lumbar spinal cord regions, and at least two from the sacral region, as well as extensive sampling of the brain, spinal cord, and selected peripheral nerves. Peripheral nerve sampling differed slightly for the nine studies but generally included a combination of nerves from the hindlimb (common peroneal, tibial, sural, and/or sciatic) and/or forelimb (radial and/or ulnar).

Characterization of microscopic (histopathologic) findings

The meta-analysis reported in this publication was limited to test article-related findings of neuronal degeneration, necrosis, and/or loss, as well mononuclear cell inflammation in the DRG and TG; to axon degeneration and/or mononuclear cell infiltrate in the spinal cord and/or peripheral nerves, excluding background findings; and to test article-related findings in other tissues and organ systems, although a complete microscopic evaluation was conducted according to the protocol and reported for each study. Within the DRG, mononuclear cell inflammation was characterized by variable and increased numbers of mononuclear cells generally associated with neuronal cell body degeneration and/or the presence of cellular debris. Neuronal necrosis was characterized by small and/or irregularly shrunken neuronal cell bodies with scalloped borders and an indistinct or absent nucleus with or without cellular debris, typically surrounded by mononuclear cells. Neuronal degeneration was observed in a continuum with neuronal necrosis but was characterized by small and/or irregularly shrunken neuronal cell bodies with an intact nucleus that sometimes contained clumped chromatin, often surrounded by plump satellite glial cells and/or a cuff of mononuclear cells. Neuron cell loss was characterized by enlarged, irregularly oval or cuboidal satellite glial cell aggregates that filled in the area of the missing or lost neuronal cell body or surrounded a smudged eosinophilic space in which the soma had been.

In the DRG, TG, spinal cord, or peripheral nerve, axon degeneration was characterized variably by one or more of the following: irregularly dilated spaces (formerly occupied by myelin sheaths and axons) that were empty or contained swollen axons, cellular debris, and/or so-

called digestion chambers (macrophages with intracellular myelin debris). In contrast with mononuclear inflammation associated with tissue damage, mononuclear cell infiltrate was characterized by small, loose clusters of small, dark mononuclear cells that generally distributed randomly in the cell-rich area of the ganglia or in the axonal region, often near a small blood vessel.

Histopathology grading severity was applied according to test facility standard operating procedures and in accordance with the Society of Toxicologic Pathology Scientific and Regulatory Policy Committee Points to Consider publication by Schafer et al.³² A 5-point grading scale (1, minimal; 2, slight; 3, moderate; 4, marked; 5, severe) was applied using International Harmonization of Nomenclature and Diagnostic Criteria–recommended terminology in a standard toxicology data collection system (Pristima version 7.4.2 by Xybion, Princeton, NJ).

Microscopic evaluations were conducted by a trained and qualified American College of Veterinary Pathologists (ACVP) board-certified pathologist experienced in toxicologic pathology and neuropathology. Contemporaneous GLP or non-GLP pathology peer review was conducted on all nine studies by a trained and qualified ACVP board-certified pathologist experienced in toxicologic pathology and neuropathology. Pathology microscopic findings, including severity, reflected consensus between the study pathologist and the peer review pathologist.

Quanterix NfL assay

NfL assay performance was determined in serum, plasma, and CSF. K2-EDTA plasma and serum samples collected from a cephalic or femoral vein and CSF samples collected from the lumbar region and/or cisterna magna were received and stored frozen at -80°C . Serum/plasma and CSF samples were thawed and analyzed at 4- and 100-fold dilution (or 8- and 200-fold when repeat analyses were required for values above the limits of detection), respectively, for NfL using the qualified Simoa NF-light immunoassay according to the manufacturer's instructions (Cat. #103186; Quanterix, Lexington, MA). Quantification was performed on the Quanterix Simoa SR-X Analyzer, and data were analyzed using SoftMax Pro v5.4.1 (Molecular Devices, Sunnyvale, CA). Values above or below the limit of quantitation were uncommon. For the purpose of the meta-analysis, values that were below the limit of quantitation were reported as the lower limit of quantitation (LLoQ)/2. If the pre-dose value was below the limit of quantitation, the LLoQ/2 was used to calculate the fold change compared with pre-dose. If the post-dose value also was below the limit of quantitation, the fold change was reported as one. Laboratory results in Standard for Exchange of Nonclinical Data (SEND) format are provided in [Table S7](#), with extensions indicating results below, within, or above the limit of quantitation denoted with qualifiers "<, =, >".

Data extraction and analyses

Quality-controlled raw data for NfL and histopathology were extracted from the Novartis study data warehouse in the SEND

format (Tables S2, S7–S8). Data from nine AAV9 nonclinical studies (four GLP and five non-GLP) were extracted and aggregated into quality-checked versus the finalized study reports. Statistical analyses were performed using R software version 3.6.1 (<https://www.r-project.org>). Histopathology severity of microscopic findings was graded as described. For the purposes of the analysis, tissues designated as not remarkable (“dashed” in the Pristima data collection system) were coded numerically as 0.

Because analysis of matrices, such as blood or CSF, are a sum of changes within multiple DRGs, the method of comparison incorporated evaluation procedures that account for the maximum severity of injury from multiple areas of evaluated tissue. Therefore, for the purposes of the meta-analysis to assess the usefulness of NFL, the maximum severity for each animal was determined based on microscopic evaluation of several DRG (n = 18–21/animal) collected from spinal cord regions/segments corresponding to cervical, thoracic, or lumbar regions (n = 5 or 6 from each region) and the sacral region (n = 2 or 3). A composite histology endpoint was created for each animal, reporting the maximum severity grade for each of the following findings.

- MISTRESC (microscopic findings)
 - Aggregate, satellite cells/neuronal loss
 - egeneration/necrosis
 - Glial cell, increased/neuronal cell loss
- MISPEC (tissues)
 - Ganglion, dorsal root and ganglion, trigeminal

Each animal was assigned a single grade for the composite endpoint: 132 unremarkable, 67 minimal, 41 slight, and 20 moderate, totaling 260 animals with DRG outcomes defined (Table S3).

Terminal NFL concentrations in blood and CSF were correlated with composite DRG maximum severity grade (the composite endpoint described above), after excluding six animals for which terminal NFL concentrations were not available. The R library pROC package was used for ROC analysis of NFL versus DRG composite histology endpoint outcome. Animals having a maximum severity grade of minimal or greater were classified as positives, whereas animals graded as unremarkable were classified as negatives. To account for potential confounders, logistic regression was used to create a base model of DRG outcome, using several categorical variables (being in a control group – 2 level, sex – 2 level, route – 3 level) and dose. Only one variable coding for the LP route had a coefficient (nearly) reaching significance for inclusion in the model (p = 0.06). This base model tested whether NFL concentrations were significantly correlated with the outcome, after removing variation explained by the potential confounders.

The base model was expanded in two steps: first by adding blood NFL-to-pre-dose ratio and second by adding CSF NFL-to-pre-dose ratio as variables to the base model. Because these variables were correlated, their significance in the model was evaluated by comparing re-

siduals of the expanded model versus base model using a χ^2 test (using the add1 R function with test = “Chisq”).

DATA AVAILABILITY

All data generated or analyzed during this study are included in this published article (and its Supplemental information files).

SUPPLEMENTAL INFORMATION

Supplemental information can be found online at <https://doi.org/10.1016/j.omtm.2022.12.012>.

ACKNOWLEDGMENTS

The authors acknowledge the expertise of David Kagan and Laura Beasley-Topliffe in the analysis and quality assurance of NFL data for extraction from the Novartis study data warehouse.

Editorial support was provided by Jennifer Gibson, PharmD, of Kay Square Scientific, Newtown Square, PA. Funded by Novartis Gene Therapies, Inc.

AUTHOR CONTRIBUTIONS

E.W.J., J.J.S., E.M., C.M., D.H.C., F.F.T., E.H., and K.P. all contributed to the study collection and design, data collection and analysis, review of the manuscript, and revision and approval of the final version of the manuscript.

DECLARATION OF INTERESTS

E.M., C.M., D.H.C., and F.F.T. are employees of Novartis Pharmaceuticals Corporation, East Hanover, NJ. E.W.J., J.J.S., E.H., and K.P. are employees of Novartis Institutes for BioMedical Research, Cambridge, MA. All authors own Novartis stock or other equities.

REFERENCES

1. Fader, K.A., Pardo, I.D., Kovi, R.C., Soms, C.J., Wang, H.H., Vaidya, V.S., Ramaiah, S.K., and Sirlivelu, M.P. (2022). Circulating neurofilament light chain as a promising biomarker of AAV induced dorsal root ganglion toxicity in nonclinical toxicology species. *Mol. Ther. Methods Clin. Dev.* 25, 264–277.
2. Hinderer, C., Katz, N., Buza, E.L., Dyer, C., Goode, T., Bell, P., Richman, L.K., and Wilson, J.M. (2018). Severe toxicity in nonhuman primates and piglets following high-dose intravenous administration of an adeno-associated virus vector expressing human SMN. *Hum. Gene Ther.* 29, 285–298.
3. Hordeaux, J., Buza, E.L., Dyer, C., Goode, T., Mitchell, T.W., Richman, L., Denton, N., Hinderer, C., Katz, N., Schmid, R., et al. (2020). Adeno-associated virus-induced dorsal root ganglion pathology. *Hum. Gene Ther.* 31, 808–818.
4. Tukov, F.F., Mansfield, K., Milton, M., Meseck, E., Penraat, K., Chand, D., and Hartmann, A. (2022). Single-dose intrathecal dorsal root ganglia toxicity of onasemnogene ABEARVOVEC in cynomolgus monkeys. *Hum. Gene Ther.* 33, 740–756. <https://doi.org/10.1089/hum.2021.255>.
5. Li, C.-L., Li, K.-C., Wu, D., Chen, Y., Luo, H., Zhao, J.-R., Wang, S.-S., Sun, M.-M., Lu, Y.-J., Zhong, Y.-Q., et al. (2016). Somatosensory neuron types identified by high-coverage single-cell RNA-sequencing and functional heterogeneity. *Cell Res.* 26, 83–102.
6. Li, C.-L., Li, K.-C., Wu, D., Chen, Y., Luo, H., Zhao, J.-R., Wang, S.-S., Sun, M.-M., Lu, Y.-J., Zhong, Y.-Q., et al. (2016). Erratum: somatosensory neuron types identified by high-coverage single-cell RNA-sequencing and functional heterogeneity. *Cell Res.* 26, 967.
7. Abram, S.E., Yi, J., Fuchs, A., and Hogan, Q.H. (2006). Permeability of injured and intact peripheral nerves and dorsal root ganglion. *Anesthesiology* 105, 146–153.

8. Godel, T., Pham, M., Heiland, S., Bendszus, M., and Bäumer, P. (2016). Human dorsal-root-ganglion perfusion measured in-vivo by MRI. *Neuroimage* *141*, 81–87.
9. Haberberger, R.V., Barry, C., Dominguez, N., and Matusica, D. (2019). Human dorsal root ganglion. *Front. Cell. Neurosci.* *13*, 271.
10. Jimenez-Andrade, J.M., Herrera, M.B., Ghilardi, J.R., Vardanyan, M., Melemedjian, O.K., and Mantyh, P.W. (2008). Vascularization of the dorsal root ganglia and peripheral nerve of the mouse implications for chemical-induced peripheral sensory neuropathies. *Mol. Pain* *4*, 10.
11. Hanani, M., and Spray, D.C. (2020). Emerging importance of satellite glia in nervous system function and dysfunction. *Nat. Rev. Neurosci.* *21*, 485–498.
12. Butt, M.T. (2020). Sampling and evaluating the peripheral nervous system. *Toxicol. Pathol.* *48*, 10–18.
13. Gordon, B.A. (2020). Neurofilaments in disease: what do we know? *Curr. Opin. Neurobiol.* *61*, 105–115.
14. Khalil, M., Teunissen, C.E., Otto, M., Piehl, F., Sormani, M.P., Gattringer, T., Barro, C., Kappos, L., Comabella, M., Fazekas, F., et al. (2018). Neurofilaments as biomarkers in neurological disorders. *Nat. Rev. Neurol.* *14*, 577–589.
15. Kuhle, J., Barro, C., Andreasson, U., Derfuss, T., Lindberg, R., Sandelius, Å., Liman, V., Norgren, N., Blennow, K., and Zetterberg, H. (2016). Comparison of three analytical platforms for quantification of the neurofilament light chain in blood samples: ELISA, electrochemiluminescence immunoassay and Simoa. *Clin. Chem. Lab. Med.* *54*, 1655–1661.
16. Gaetani, L., Paolini Paoletti, F., Bellomo, G., Mancini, A., Simoni, S., Di Filippo, M., and Parnetti, L. (2020). CSF and blood biomarkers in neuroinflammatory and neurodegenerative diseases: implications for treatment. *Trends Pharmacol. Sci.* *41*, 1023–1037.
17. Gafson, A.R., Barthélemy, N.R., Bomont, P., Carare, R.O., Durham, H.D., Julien, J.-P., Kuhle, J., Leppert, D., Nixon, R.A., Weller, R.O., et al. (2020). Neurofilaments: neurobiological foundations for biomarker applications. *Brain* *143*, 1975–1998.
18. Lee, M.K., Xu, Z., Wong, P.C., and Cleveland, D.W. (1993). Neurofilaments are obligate heteropolymers in vivo. *J. Cell Biol.* *122*, 1337–1350.
19. Andersson, E., Janelidze, S., Lampinen, B., Nilsson, M., Leuzy, A., Stomrud, E., Blennow, K., Zetterberg, H., and Hansson, O. (2020). Blood and cerebrospinal fluid neurofilament light differentially detect neurodegeneration in early Alzheimer's disease. *Neurobiol. Aging* *95*, 143–153.
20. Kapoor, M., Foiani, M., Heslegrave, A., Zetterberg, H., Lunn, M.P., Malaspina, A., Gillmore, J.D., Rossor, A.M., and Reilly, M.M. (2019). Plasma neurofilament light chain concentration is increased and correlates with the severity of neuropathy in hereditary transthyretin amyloidosis. *J. Peripher. Nerv. Syst.* *24*, 314–319.
21. Kim, S.-H., Choi, M.K., Park, N.Y., Hyun, J.-W., Lee, M.Y., Kim, H.J., Jung, S.K., and Cha, Y. (2020). Serum neurofilament light chain levels as a biomarker of neuroaxonal injury and severity of oxaliplatin-induced peripheral neuropathy. *Sci. Rep.* *10*, 7995.
22. Meregalli, C., Fumagalli, G., Alberti, P., Canta, A., Carozzi, V.A., Chiorazzi, A., Monza, L., Pozzi, E., Sandelius, Å., Blennow, K., et al. (2018). Neurofilament light chain as disease biomarker in a rodent model of chemotherapy induced peripheral neuropathy. *Exp. Neurol.* *307*, 129–132.
23. Meregalli, C., Fumagalli, G., Alberti, P., Canta, A., Chiorazzi, A., Monza, L., Pozzi, E., Carozzi, V.A., Blennow, K., Zetterberg, H., et al. (2020). Neurofilament light chain: a specific serum biomarker of axonal damage severity in rat models of chemotherapy-induced peripheral neurotoxicity. *Arch. Toxicol.* *94*, 2517–2522.
24. Olsson, B., Portelius, E., Cullen, N.C., Sandelius, Å., Zetterberg, H., Andreasson, U., Höglund, K., Irwin, D.J., Grossman, M., Weintraub, D., et al. (2019). Association of cerebrospinal fluid neurofilament light protein levels with cognition in patients with dementia, motor neuron disease, and movement disorders. *JAMA Neurol.* *76*, 318–325.
25. Boehnke, S.E., Robertson, E.L., Armitage-Brown, B., Wither, R.G., Lyra e Silva, N.M., Winterborn, A., Levy, R., Cook, D.J., De Felice, F.G., and Munoz, D.P. (2020). The effect of lumbar puncture on the neurodegeneration biomarker neurofilament light in macaque monkeys. *Alzheimers Dement.* *12*, e12069.
26. Hordeaux, J., Buza, E.L., Jeffrey, B., Song, C., Jahan, T., Yuan, Y., Zhu, Y., Bell, P., Li, M., Chichester, J.A., et al. (2020). MicroRNA-mediated inhibition of transgene expression reduces dorsal root ganglion toxicity by AAV vectors in primates. *Sci. Transl. Med.* *12*, eaba9188.
27. Buss, N., Lanigan, L., Zeller, J., Cissell, D., Metea, M., Adams, E., Higgins, M., Kim, K.H., Budzynski, E., Yang, L., et al. (2022). Characterization of AAV-mediated dorsal root ganglionopathy. *Mol. Ther. Methods Clin. Dev.* *24*, 342–354.
28. Alves, C.R.R., Petrillo, M., Spellman, R., Garner, R., Zhang, R., Kiefer, M., Simeone, S., Sohn, J., Eichelberger, E.J., Rodrigues, E., et al. (2021). Implications of circulating neurofilaments for spinal muscular atrophy treatment early in life: a case series. *Mol. Ther. Methods Clin. Dev.* *23*, 524–538.
29. Day, J.W., Mendell, J.R., Mercuri, E., Finkel, R.S., Strauss, K.A., Kleyn, A., Tauscher-Wisniewski, S., Tukov, F.F., Reyna, S.P., and Chand, D.H. (2021). Clinical trial and postmarketing safety of onasemnogene abeparvovec therapy. *Drug Saf.* *44*, 1109–1119.
30. Khalil, M., Pirpamer, L., Hofer, E., Voortman, M.M., Barro, C., Leppert, D., Benkert, P., Ropele, S., Enzinger, C., Fazekas, F., et al. (2020). Serum neurofilament light levels in normal aging and their association with morphologic brain changes. *Nat. Commun.* *11*, 812.
31. Yuan, A., and Nixon, R.A. (2021). Neurofilament proteins as biomarkers to monitor neurological diseases and the efficacy of therapies. *Front. Neurosci.* *15*, 689938.
32. Schafer, K.A., Eighmy, J., Fikes, J.D., Halpern, W.G., Hukkanen, R.R., Long, G.G., Meseck, E.K., Patrick, D.J., Thibodeau, M.S., Wood, C.E., and Francke, S. (2018). Use of severity grades to characterize histopathologic changes. *Toxicol. Pathol.* *46*, 256–265.